Production of nuclides with $43 \leq A \leq 51$ in the interaction of 1–28.5 GeV protons with V, Ag, In, Pb, and U targets*

Y. Y. Chu, G. Friedlander, and L. Husain†
Chemistry Department, Brookhaven National Laboratory, Upton, New York 11973
(Received 18 August 1976)

The production cross sections of nuclides ranging from ^{43}Sc to ^{51}Cr in the interaction of 1–28.5 GeV protons with vanadium, silver, indium, lead, and uranium have been measured. Excitation functions of the weighted average of the measured yields for these targets are shown. Charge dispersion curves have been deduced from the measured results and total isobaric yields evaluated by using a nonlinear least squares program. Starting from the premise that spallation is chiefly responsible for the production of these nuclides from vanadium, the systematic trends thus derived suggest that these nuclides cannot be produced from heavy targets (lead and uranium) by either fission or spallation alone. Our results are not sufficient, however, to distinguish whether these nuclides are produced via some exotic process such as fragmentation or by a combination of more conventional mechanisms.

[NUCLEAR REACTIONS Targets: natural V, Ag, In, Pb, and U; projectiles: 1–28.5 GeV protons, measured $\sigma(A, Z)$, 14 products ^{43}Sc–^{51}Cr; excitation functions of weighted average of measured yields, deduced charge dispersion curves, and total isobaric yield for $A=47$. Chemically separated Ca, Sc, V, and Cr samples.]

I. INTRODUCTION

Among the nuclides produced in the interaction of GeV protons with heavy elements, the mass region of $A \sim 50$ occupies a unique and inherently interesting position. For sub-GeV proton energies, the yield[1-4] decreases to very low values at $A \sim 50$ and $A \sim 160$ but upturns toward both the very light masses ($A < 30$) and the target. Thus the measured mass yield curves have deep valleys at $A \lesssim 50$ and $A \gtrsim 160$, with the typical low-energy fission mass range in the middle and the very light fragments and the spallation products near the target on both ends. Even though there are significant changes for the individual yields in the fission mass range with varying energy (as evidenced, e.g., by the broadening of the charge dispersion curve with increasing bombarding energy[5,6] and by differences in the shapes of excitation functions for a number of nuclides[6]) the overall mass-yield curves[1-4] are rather insensitive to the bombarding energy in this energy region. However, the yields[7-10] for nuclides at $A \lesssim 50$ and $A \gtrsim 160$ increase by an order of magnitude or more as the proton energy rises from several hundred MeV to several GeV. These observations coincide with other changes over the same energy range: The rapid increases in the yields[6,11-13] of neutron-deficient nuclides in the fission mass region and a decrease in the ranges[10,11,14-18] of these same species to about one-half of their values at several hundred MeV proton energy.

It is well established from counter experiments[19,20] that the yields of products with $A \sim 50$ in the interaction of 2.9 GeV protons with uranium and bismuth cannot be accounted for by binary-fission processes. However, just what mechanism or combination of mechanisms are involved in the formation of these products at multi-GeV energies is still unclear. Counter experiments[21-23] designed to look for the light fragments and their coincident partners produced in the interaction of 28 GeV protons with uranium and gold should be most useful in elucidating the mechanism(s) responsible. The counter telescope system used can resolve elements up to $Z \approx 24$,[22] i.e., $A \sim 50$. However, the results from the coincidence experiments are still not available.

There have been several investigations[8-10,24,25] of yields in the $A \lesssim 50$ region (particularly Sc yields) from the interaction of GeV protons with heavy element targets as well as a number of studies[25-30] on light and medium targets. It has been demonstrated[30] that the yields in the mass region $37 \leq A \leq 64$ from copper (a typical light target) can be expressed in simple analytical form and the parameters can be optimized by using a nonlinear least squares program. Since the β-stability valley is relatively narrow in the $A \sim 50$ region, charge dispersion (CD) curves may be expected to retain the same general shape independent of target and bombarding energy, with only slight changes in width and peak position, so that the yields from heavy targets can presumably be analyzed in terms of the same general analytical form used for light targets.

The results reported in this paper include yields of 14 nuclides from ^{43}Sc to ^{51}Cr (with most of the results on scandium isotopes) from the interaction of 1–28.5 GeV protons with five different targets ranging from vanadium to uranium. The data can be divided into two groups: those from the light and medium targets (V, Ag, and In) and those from the heavy targets (Pb and U). These results reveal some systematic trends which in turn may shed light on our understanding of the formation of these nuclides from the interaction of GeV protons with heavy targets.

II. EXPERIMENTAL TECHNIQUES AND RESULTS

A. Irradiations

Irradiations were performed in the circulating beams of the Brookhaven Cosmotron (for 1, 2, and 3 GeV) and the Brookhaven Alternating Gradient Synchrotron (AGS, for 3, 6, 10, 18, and 28.5 GeV). The lengths of irradiations ranged from several minutes to two hours. Standard target assemblies[26] for Cosmotron and AGS were used. These assemblies consisted of a 25 μm (or 50 μm) thick target foil sandwiched between two stacks of three 25 μm aluminum foils. For vanadium, silver, and indium targets, three target foils were used, only the middle one being used for chemical processing and the other two serving as guard foils. Identical areas for the target and the aluminum monitor foils were punched out after the irradiation. The target piece and the central aluminum piece were weighed in order to determine the numbers of target and aluminum nuclei irradiated. The ^{24}Na activity produced in the aluminum foil by ^{27}Al$(p, 3pn)^{24}$Na reaction was later measured and served to monitor the proton beam intensity in all irradiations. The monitor cross sections (in mb) used[31] are 10.5 for 1 GeV, 9.5 for 2 GeV, 9.1 for 3 GeV, 8.7 for 6 GeV, 8.6 for 10, 18, and 28.5 GeV.

B. Chemical separations

Chemical separations[32] were carried out for all the experiments described. Special attention was given to the decontamination steps for uranium targets because of the relatively large cross sections in the fission mass range. For example, calcium was carefully decontaminated from barium and strontium by means of fuming nitric acid precipitations; scandium was purified from rare earths and yttrium by the fluoride complex formation of the former. Determinations of yields of the chemical separations were performed after the completion of the radioactivity assays.

C. Radioactivity measurements

Relevant nuclear properties of the nuclides studied are listed in Table I. Early γ-ray measurements on Pb and U targets at 1, 2, and 3 GeV (Cosmotron energies) were made with NaI(Tl) detectors and most of the later measurements at AGS energies (3 GeV and higher) were made with Ge(Li) detectors. Whenever the measurements were repeated with Ge(Li) detectors, the agreement with earlier results using NaI(Tl) detectors was almost always within experimental uncertainties of $\pm 15\%$, thus lending confidence to all the earlier results obtained with NaI(Tl) detectors. Losses in photopeak intensities due to summing of coincident radiations were corrected for whenever applicable. The Ti K x rays from ^{49}V were assayed on a large gas proportional counter with a thin Be window. The β-activity measurements were made using end-window proportional counters. Because of the low β energy in ^{45}Ca, self-absorption corrections were made for all ^{45}Ca measurements using empirically determined curves. The efficiencies of the detectors were determined using calibrated radioactive standards. Samples were counted over sufficiently long periods of time to assure correct decay behavior and all decay curves were resolved using the *CLSQ* program.[35]

The cross sections for scandium nuclides ob-

TABLE I. Relevant properties of the measured nuclides. Data selected from Ref. 33, Ref. 34, and recent literature values.

Nuclide	$t_{1/2}$	Radiation	Energy (MeV)	Abundance
^{45}Ca	164 day	β^-	0.257	1.00
^{47}Ca	4.53 day	γ	1.297	0.74
^{43}Sc	3.89 h	γ	0.511	1.76
^{44}Sc	3.90 h	γ	0.511	1.88
			1.159	1.00
^{44}Sc^m	2.44 day	γ	0.271	0.88
^{46}Sc	83.9 day	γ	0.889	1.00
			1.120	1.00
^{47}Sc	3.40 day	γ	0.160	0.70
^{48}Sc	43.67 h	γ	0.984	1.00
			1.038	0.98
			1.314	1.00
^{49}Sc	57.5 min	β^-	2.01	1.00
^{47}V	32.0 min	γ	0.511	1.92
^{48}V	16.1 day	γ	0.984	1.00
			1.314	1.00
^{49}V	300 day	Ti K x ray	0.0045	0.158
^{48}Cr	24 h	γ	0.116	0.98
			0.309	0.99
^{49}Cr	41.9 min	γ	0.511	1.86
^{51}Cr	27.8 day	γ	0.320	0.098

tained from vanadium, silver, and indium targets at several energies are given in Table II. The results for nuclides with $43 \leq A \leq 51$ obtained from lead and uranium targets at different proton energies are listed in Table III. With the exception of the results for 10 and 18 GeV proton bombardments of silver in Table II, all entries represent averages based on two or more runs. The errors quoted include counting statistics, uncertainties in counter efficiencies, chemical yield determinations, and summing corrections. The uncertainties of the radiation abundances and the monitor cross sections are not reflected therein. Corrections for the contributions of secondary particles to ^{24}Na production in the monitor foils were made only for Pb and U targets at 3 and 28.5 GeV proton energies. Correction factors per 100 mg/cm^2 target thickness are 3.5%[36] and 4%[36] for Pb and U targets at 3 GeV, respectively and 14%[37] for both Pb and U targets at 28.5 GeV.

In general, the agreement between replicate runs is better than the experimental uncertainties. Whenever the standard deviation of the individual measurements from the mean exceeds the experimental uncertainty, the former is quoted as error.

The results obtained in this work were compared with those from earlier investigations whenever such comparison could be made. The agreement between the results from this work and from Ref. 26 on vanadium interactions with 28.5 GeV protons demonstrates that direct counting using high-resolution γ spectroscopy for light targets can give results indistinguishable from those obtained with chemically separated samples. Our 28.5 GeV results on silver agree with those of Ref. 27 within experimental uncertainties; the ^{47}Sc and ^{48}Sc yields from silver at 11.5 GeV (Ref. 28) are higher than our results at 10 and 18 GeV, and their yields at 300 GeV (Ref. 29) are slightly higher than our results at 28.5 GeV. The agreement between our data and earlier results on Pb (Ref. 24) and U (Refs. 10 and 24) is not uniformly good even though more than two-thirds of the comparisons are within experimental uncertainties. Considering that different counting techniques were employed in these investigations, and irradiations were carried out at three different accelerators (ZGS at Argonne, Cosmotron and AGS at Brookhaven) over a span of many years, the overall agreement should be considered reasonable. Even in the worst cases, the differences are usually only two or three standard deviations.

III. DISCUSSION

A. Excitation functions

Inspection of the cross sections in Tables II and III shows that the excitation functions for all products investigated rose much more steeply with Pb and U as targets than with Ag. Using in addition the published results for 3 GeV (Ref. 26) protons on V, 3.9 GeV (Ref. 30) and 28.5 GeV (Ref. 38) protons on Cu, and 3 GeV (Ref. 27) protons on Ag, we have constructed *average* excitation functions as follows: For each product nuclide and each target element, the cross section at every energy was evaluated relative to that at 3 GeV taken as unity. The weighted average of these relative cross sections for all measured nuclides was then calculated for each energy-target combination. The results are listed in Table IV.

For vanadium as a target, the average mass yield in this mass region appears to be slightly lower at 28.5 GeV than at 3 GeV, as was already shown in a different way by the comparison of the mass-yield curves at these two energies in Ref. 26. The same trend is observed for copper as a target between 3.9 and 28.5 GeV. For the silver target, the average mass yield curve for this portion rises slowly between 3 and 28.5 GeV. As already mentioned, the lead and uranium excitation functions rise over the entire energy range, with the increase between 1 and 3 GeV being somewhat steeper for lead than for uranium.

The observations for vanadium, copper, and silver targets are all consistent with the usual spallation mechanism: The nuclear cascades tend to be somewhat longer and the excitation energies

TABLE II. Scandium cross sections in millibarns from vanadium, silver, and indium targets.

Nuclide	Type of yield[a]	V target $E_p = 28.5$ GeV	Ag target $E_p = 6$ GeV	Ag target $E_p = 10$ GeV	Ag target $E_p = 18$ GeV	Ag target $E_p = 28.5$ GeV	In target $E_p = 28.5$ GeV
^{43}Sc	C	2.18 ± 0.22	0.72 ± 0.08	•••	0.68 ± 0.08	0.89 ± 0.08	0.57 ± 0.06
^{44}Sc	I	4.95 ± 0.45	1.07 ± 0.10	•••	•••	1.21 ± 0.12	0.95 ± 0.09
^{44}Sc^m	I	4.40 ± 0.44	2.00 ± 0.20	1.88 ± 0.20	2.07 ± 0.22	2.13 ± 0.21	1.62 ± 0.16
^{46}Sc	I	14.4 ± 1.40	2.79 ± 0.28	2.79 ± 0.30	3.10 ± 0.30	3.04 ± 0.30	2.96 ± 0.30
^{47}Sc	I	10.2 ± 1.00	1.62 ± 0.16	1.56 ± 0.16	1.70 ± 0.17	1.44 ± 0.14	1.59 ± 0.16
^{48}Sc	I	4.32 ± 0.43	0.37 ± 0.04	0.37 ± 0.05	0.41 ± 0.05	0.44 ± 0.04	0.48 ± 0.05

[a] I means independent; C means cumulative.

TABLE III. Cross sections in millibarns for $43 \leq A \leq 51$ from lead and uranium targets.

Nuclide	Type of yield[a]	Pb target $E_p = 1$ GeV	Pb target $E_p = 2$ GeV	Pb target $E_p = 3$ GeV	Pb target $E_p = 28.5$ GeV	U target $E_p = 1$ GeV	U target $E_p = 2$ GeV	U target $E_p = 3$ GeV	U target $E_p = 28.5$ GeV
^{45}Ca	C	0.26 ± 0.04	0.62 ± 0.10	1.39 ± 0.20	3.25 ± 0.35	1.42 ± 0.20	2.59 ± 0.26	3.50 ± 0.50	11.21 ± 0.70
^{47}Ca	C	0.068 ± 0.010	0.15 ± 0.02	0.26 ± 0.04	0.56 ± 0.06	0.35 ± 0.05	0.80 ± 0.08	0.94 ± 0.10	2.01 ± 0.14
^{43}Sc	C	...	0.18 ± 0.07	0.29 ± 0.11	0.46 ± 0.05	0.12 ± 0.03	0.26 ± 0.07	0.51 ± 0.13	0.96 ± 0.10
^{44}Sc	I	...	0.06 ± 0.03	0.10 ± 0.04	0.71 ± 0.07	0.0056 ± 0.002	0.079 ± 0.020	0.21 ± 0.07	0.32 ± 0.03
^{44}Sc^{m}	I	0.08 ± 0.02	0.16 ± 0.03	0.47 ± 0.09	1.21 ± 0.13	0.066 ± 0.013	0.33 ± 0.05	0.56 ± 0.10	1.57 ± 0.17
^{46}Sc	I	0.57 ± 0.09	0.75 ± 0.11	1.67 ± 0.25	3.90 ± 0.44	1.17 ± 0.16	2.41 ± 0.24	4.03 ± 0.40	7.70 ± 0.34
^{47}Sc	I	0.19 ± 0.04	0.87 ± 0.12	2.02 ± 0.31	3.16 ± 0.30	1.23 ± 0.16	3.00 ± 0.30	3.57 ± 0.35	5.98 ± 0.50
^{48}Sc	I	0.14 ± 0.025	0.35 ± 0.05	0.68 ± 0.10	1.30 ± 0.13	0.88 ± 0.13	1.52 ± 0.14	1.55 ± 0.14	3.10 ± 0.21
^{49}Sc	C	0.16 ± 0.03	0.30 ± 0.06	1.27 ± 0.25	...	0.89 ± 0.13	1.20 ± 0.18	1.94 ± 0.28	...
^{47}V	C	0.039 ± 0.010	0.096 ± 0.02	0.33 ± 0.08	0.43 ± 0.04	0.10 ± 0.02	0.31 ± 0.06	1.13 ± 0.22	0.23 ± 0.02
^{48}V	I	...	0.48 ± 0.11	0.36 ± 0.09	1.99 ± 0.19	0.31 ± 0.04	0.38 ± 0.05	0.49 ± 0.07	2.34 ± 0.24
^{49}V	C	...	...	...	...	2.08 ± 1.03	2.60 ± 1.03	4.04 ± 1.61	...
^{48}Cr	C	...	...	...	...	0.00046 ± 0.00021	0.0046 ± 0.0021	0.0079 ± 0.0040	...
^{49}Cr	C	...	...	...	...	0.049 ± 0.011	0.063 ± 0.013	0.074 ± 0.015	...
^{51}Cr	C	...	0.60 ± 0.18	1.15 ± 0.23	...	1.11 ± 0.22	1.41 ± 0.21	2.31 ± 0.35	...

[a] I means independent; C means cumulative.

higher at 28.5 GeV than at 3 GeV, resulting in a shift of the mass yield curve toward lower masses. In the case of V and Cu bombardments, the mass region investigated here is sufficiently close to the target mass so that this trend leads to a drop in cross sections with increasing energy, while it has been established that, for silver as a target, the 28.5 GeV mass yield curve[27] crosses over the 3 GeV curve at just below $A = 60$ so that the average relative yield for our mass range is slightly higher at 28.5 GeV than at 3 GeV. The steeper slope between 1 and 3 GeV for lead than for uranium suggests a higher threshold in producing these nuclides in lead.

It is worth noting that the shapes of the excitation functions reported here for lead and uranium targets are qualitatively similar to the energy dependence of single-track events observed in mica track detector studies[39] of bismuth and uranium interactions with GeV energy protons, whereas the binary fission cross sections observed in these studies decrease monotonically as the proton energy is increased from 1 to 28.5 GeV.

B. Charge dispersion curves

The choice of an appropriate abscissa (the charge scale) in a CD curve for this mass region is complicated by the close proximity of the $N = 20, 28$ and $Z = 20$ shells. The conventional choices of $(Z_A - Z)$ or N/Z are not suitable because of the shell effect on Z_A and the distortion that can be brought in on an N/Z plot over a 15% mass spread. Cumming *et al.* employed[30] a nonlinear least squares program to fit all the measured yields in this mass region from the interaction of 3.9 GeV protons with copper. They adopted the formalism first used by Rudstam[40] and assumed the relationship $\ln[\sigma(A,Z)] = Y(A) + C[Z_p(A)]$ to approximate the yield distribution. They found that simple functional forms can fit the yield equally well as those containing higher terms, and the charge dispersion part (the second term on the right-hand side of the equation) can be represented by a Gaussian joined to an exponential tail on the neutron-rich side. Thus the relationship is expressed as $\ln[\sigma(A,Z)] = [\chi_1 + \chi_2(A - 50)] + C[Z_p(A) - Z]$, with $C[Z_p(A) - Z] = \chi_5[\chi_3 + \chi_4(A - 50) - Z]^2 + N_c$ for the Gaussian and $C[Z_p(A) - Z] = \chi_5\chi_6[2(Z_p - Z) - \chi_6] + N_c$ for the exponential tail with the two joined together at $(Z_p - Z) = \chi_6$. All the parameters (χ_1 to χ_6) could be obtained from the least squares fitting program.

In view of the wide range of results (14 product nuclides from combinations of 5 targets and 7 energies) and the difficulties arising from shell effects mentioned above, it was felt that this sim-

TABLE IV. Weighted average of the measured yields ($43 \leq A \leq 51$) relative to those at 3 GeV for five different targets.

E_p (GeV)	V target	Cu target	Ag target	Pb target	U target
1.0				0.175±0.015	0.265±0.015
2.0				0.44 ±0.032	0.69 ±0.036
3.0	1.000 [a]	1.000 [b]	1.000 [c]	1.000	1.000
6.0			1.07±0.09		
10.0			1.04±0.10		
18.0			1.09±0.10		
28.5	0.92±0.045	0.865±0.008 [d]	1.14±0.09	2.41 ±0.17	2.32 ±0.11

[a] Reference 26.
[b] Reference 30. Proton energy was 3.9 GeV.
[c] Reference 27.
[d] Reference 38. The cross sections have been adjusted using 8.6 mb for the monitor cross section instead of 8.0 mb in order to be consistent with other values at 28.5 GeV.

ple, empirical approach would make it possible to examine this collection of cross section data for systematic trends. However, it is clear that one should not attach too much quantitative significance to the fitted parameters.

Figure 1 shows the CD curve obtained by using this program for vanadium bombarded with 28.5 GeV protons. Since the agreement of our scandium results and those from Ref. 26 is excellent and many data points are needed in the least squares fitting, the solid curve represents the resulting CD curve best fitted through all the available yields in this mass region from Ref. 26. The independent yields from the present study are shown as open circles and the cumulative yields shown as filled circles. The fit of the individual data points with the CD curve is, in general, within experimental uncertainties, but the yield for ^{46}Sc is low by 2 to 3 σ's not explainable by the uncertainty of Z_p. The same procedure was applied to the 3 GeV results from Ref. 26. The optimized parameters for the CD curve and their uncertainties are listed in Table V. The Z_p and full width at half maximum (FWHM) values are the same within errors at 3 and 28.5 GeV.

The results from silver at 28.5 GeV are shown in Fig. 2. In spite of the good agreement between our results and the scandium yields in Ref. 27, the filled points do not match the solid curve too well, because the solid curve again represents the best-fitted CD curve with all the available yields in this mass region from Ref. 27, not just the scandium yields. The resulting parameters for both 3 and 28.5 GeV data from Ref. 27 are also listed in Table V. Again there is no significant change in Z_p and FWHM with energy.

Now we can proceed to use this program to fit the yields from lead and uranium targets. The resulting CD curves for lead at 3 and 28.5 GeV are shown in Figs. 3(a) and 3(b), respectively; and those for uranium at these energies are shown in Figs. 4(a) and 4(b), respectively. The independent and cumulative yields are shown with the same notations as in Fig. 1. The ^{47}V and ^{49}Sc yields from both targets at 3 GeV lie considerably higher than their respective CD curves and cannot be accounted for by the contributions of their respective precursors. In general, the overall fit of the data for 28.5 GeV to the CD curves is better than for 3 GeV. The parameters thus obtained are also listed in Table V. Note that no errors

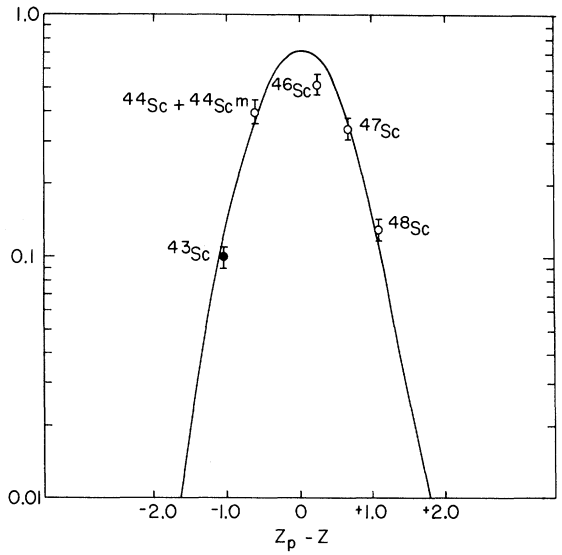

FIG. 1. Charge dispersion curve and data points for the interaction of 28.5 GeV protons and vanadium. The open circles are independent yields and the filled circles are the cumulative yields.

TABLE V. Parameters for the charge dispersion curves obtained from the least squares fitting program.

Target	E_p (GeV)	Parameters χ_3 [a]	χ_4	χ_5	χ_6	FWHM [b]
V	3	22.959±0.032	0.4270±0.0044	−1.6978±0.1094	1.0239±0.1365	1.278±0.043
	28.5	22.936±0.032	0.4264±0.0045	−1.6003±0.0971	1.0724±0.1427	1.316±0.040
Ag	3	23.235±0.034	0.4556±0.0044	−1.6723±0.0785	0.9424±0.08910	1.288±0.031
	28.5	23.307±0.040	0.4616±0.0037	−1.8057±0.0999	0.7517±0.0829	1.239±0.035
Pb	3	22.766±0.118	0.4099±0.0350	−1.2864	0.5722	1.491
	28.5	23.056±0.063	0.4799±0.0158	−1.2416±0.1142	0.7581±0.1213	1.494±0.065
U	3	22.709±0.090	0.4161±0.0281	−1.2864	0.5722	1.491
	28.5	22.778±0.131	0.4779±0.0307	−1.1504±0.2092	0.6372±0.2881	1.567±0.445

[a] $Z_p = \chi_3 + \chi_4 (A - 50)$, therefore $Z_p = \chi_3$ for $A = 50$.
[b] FWHM $= 2(-\ln 2/\chi_5)^{1/2}$, if $-\ln 2/\chi_5\chi_6 \leq \chi_6$; FWHM $= (-\ln 2/\chi_5)^{1/2} + \frac{1}{2}(-\ln 2/\chi_5\chi_6 + \chi_6)$, if $-\ln 2/\chi_5\chi_6 > \chi_6$.

are given for the χ_5 and χ_6 values for both lead and uranium at 3 GeV because the data points were only sufficient to fit four parameters instead of six, and the values for χ_5 and χ_6 were chosen to give the best overall fit.

Despite the scatter of some of the yields, it is possible to deduce the following systematic trends based on the parameters and the FWHM values listed in Table V.

(1) The value of χ_3 at 3 GeV increases (i.e., the peak of the CD curve for $A = 50$ is shifted toward higher neutron deficiency) when the target is changed from vanadium to silver. The trend is reversed in going from silver to lead and uranium

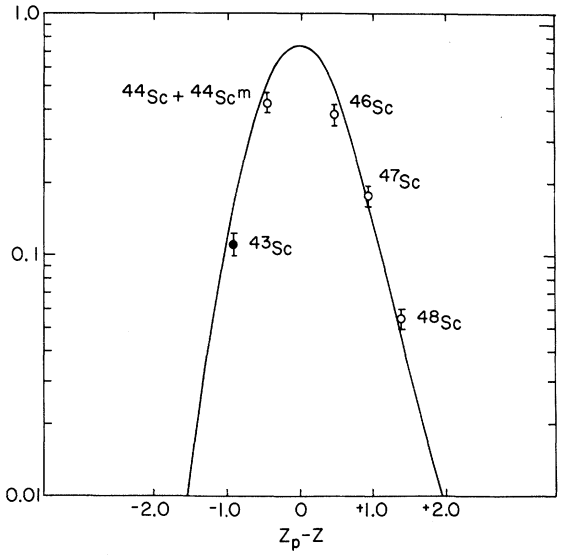

FIG. 2. Charge dispersion curve and data points for the interaction of 28.5 GeV protons and silver. Same notations are used as in Fig. 1.

targets. The same overall trend persists at 28.5 GeV among these targets.

The χ_3 value obtained in Ref. 30 for a copper target irradiated with 3.9 GeV protons is 23.419 ±0.014, slightly higher than the corresponding values for both vanadium and silver targets at 3 GeV. This suggests that the χ_3 value reaches a maximum somewhere between vanadium and silver. The shift of the peak in scandium isotopic distributions toward the neutron-rich side with increasing target mass (from yttrium to uranium) shown in Ref. 25 is in accord with this observation.

(2) The FWHM of the CD curve for vanadium and silver targets at both energies are the same within their uncertainties. The widths for lead and uranium at these energies are about the same for both targets and they are ~0.2 charge units larger than those for vanadium and silver. The extra width in the CD curves for the heavy target over the light target is on the neutron-rich side.

It should be pointed out, however, that the FWHM value is not a sensitive measure of the change in the shape of the CD curves. The significant decrease in χ_5 and χ_6 values for lead and uranium relative to the values for vanadium and silver indicates that there is not only an increase in FWHM by 0.2 charge units but also a marked decrease in the slope of the exponential tail; thus the CD curves for the higher-Z targets are distinctly more asymmetric than those for the low-Z ones. The comparison of scandium isotopic distributions from different targets in Ref. 25 also shows the same trend.

C. Total isobaric yield for $A = 47$

It is now possible to evaluate the unmeasured independent yields from the CD curves defined by

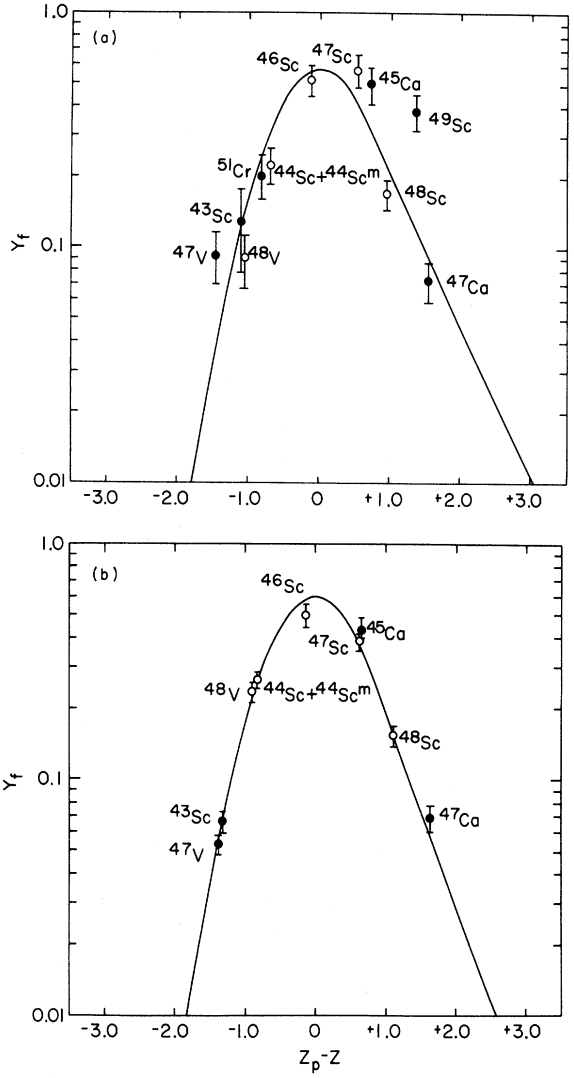

FIG. 3. (a) Charge dispersion curve and data points for the interaction of 3 GeV protons and lead. (b) Charge dispersion curve and data points for the interaction of 28.5 GeV protons and lead.

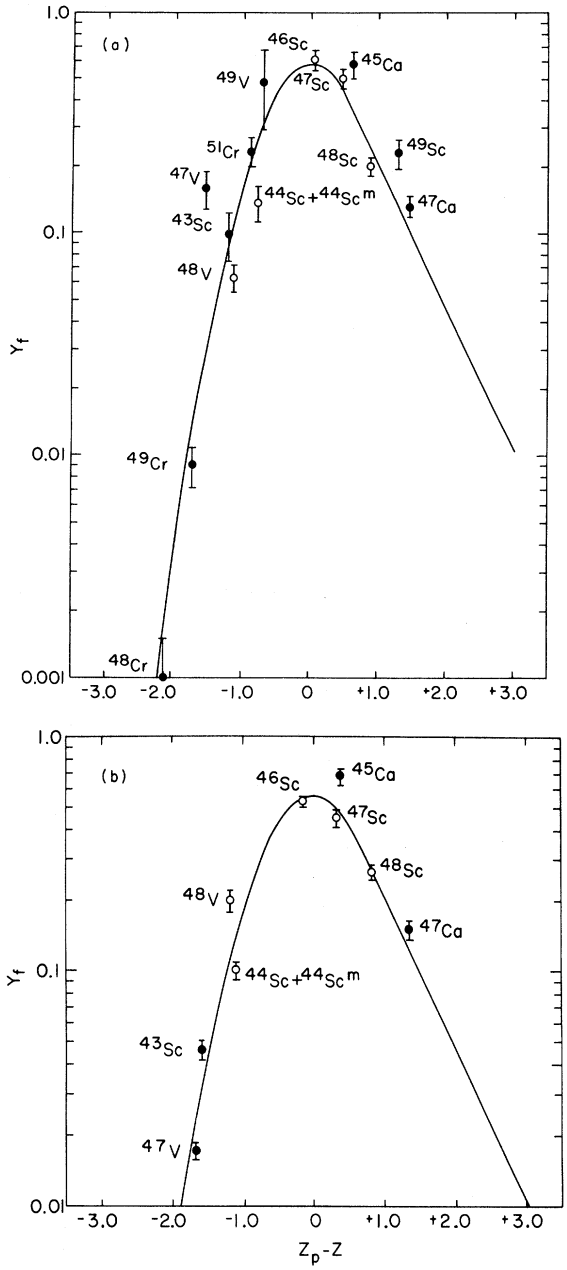

FIG. 4. (a) Charge dispersion curve and data points for the interaction of 3 GeV protons and uranium. (b) Charge dispersion curve and data points for the interaction of 28.5 GeV protons and uranium.

the parameters given in Table V and the mass yield based on the optimized χ_1 and χ_2 values. The values for χ_1 and χ_2 for different targets at various energies obtained in this work are listed in Table VI. Since only the unmeasured yield of ^{47}Ti is needed to give the total isobaric yield for $A = 47$ (except from the indium target), we have evaluated the independent yield for ^{47}Ti in all the cases from the parameters obtained in this work, and the total isobaric yields for $A = 47$ are given in the last column of Table VI. The excitation functions for the total isobaric yields at $A = 47$ are the same within uncertainties as those for the weighted average of the measured yields given in Table IV.

Both the total isobaric yields at 3 and 28.5 GeV from these four targets exhibit two branches: The yields decrease between vanadium and silver (between vanadium and indium for 28.5 GeV) and the trend reverses between lead and uranium. Similar behavior was observed before[41] for the production of ^{18}F and ^{24}Na from different targets with

TABLE VI. Parameters and total isobaric yields for $A=47$ obtained from the least squares fitting program.

Target	E_p (GeV)	χ_1	χ_2	$\sigma_{A=47}$ (mb)
V	3 [a]	3.4418 ± 0.1168	0.075 98 ± 0.011 37	33.4 ± 3.6
	28.5 [a]	3.3280 ± 0.1102	0.086 89 ± 0.011 57	30.4 ± 3.0
Ag	3 [b]	1.6396 ± 0.1149	0.040 37 ± 0.011 98	6.5 ± 0.77
	28.5 [b]	1.7973 ± 0.1127	0.005 05 ± 0.011 28	8.1 ± 0.97
In	28.5	1.0971 ± 0.2280	0.022 97 ± 0.035 83	5.1 ± 2.0
Pb	1	−0.6220 ± 0.3690	0.089 65 ± 0.115 62	0.58 ± 0.30
	2	0.4493 ± 0.1965	0.155 31 ± 0.060 84	1.9 ± 0.38
	3	1.0692 ± 0.2383	0.114 59 ± 0.068 86	4.2 ± 0.94
	28.5	1.7061 ± 0.1693	0.039 91 ± 0.036 78	8.2 ± 1.4
U	1	1.1236 ± 0.1325	0.216 86 ± 0.043 47	2.8 ± 0.37
	2	1.4026 ± 0.1173	0.125 79 ± 0.039 45	5.5 ± 0.49
	3	1.6572 ± 0.2338	0.079 14 ± 0.075 27	8.5 ± 1.7
	28.5	1.6770 ± 0.3616	−0.106 38 ± 0.087 32	12.7 ± 3.9

[a] Data taken from Ref. 26.
[b] Data taken from Ref. 27.

GeV protons. It was suggested in Ref. 41 that though spallation can easily account for the production of ^{18}F and ^{24}Na from the light targets it would not be sufficient to explain the yields of these nuclides from heavy targets. Our observation here leads to the same conclusion.

It should be pointed out that the total isobaric yield at $A = 47$ is much higher than that[42] at $A \sim 160$ for the interaction of 28.5 GeV protons with uranium. This fact also argues against spallation as the major contributor to the production of the nuclides at $A \sim 50$ because one expects the mass yields of spallation to decrease, or at the most stay flat, with increasing mass difference between product and target. Therefore phenomenologically speaking, other process(es) must be operating in addition to, or in place of, spallation.

On the other hand, from the results of earlier works,[19,20] it is evident that binary fission cannot account for the magnitude of the cross sections observed in this mass region in the interaction of GeV protons with uranium and bismuth targets. Neither can ternary fission be chiefly responsible for the production of these nuclides, because the ratio[39] of ternary to binary events in GeV proton fission of uranium and bismuth is only 10^{-2} to 10^{-3}, much too small to account for the observed cross sections.

In summary, combining the results from this study and from earlier studies, one can conclude that neither binary fission, nor ternary fission, nor spallation alone can account for the observed cross sections in this mass range from heavy targets. Whether these products are produced in a more exotic process, such as "fragmentation," in which fragments in this mass range are ejected from an unequilibrated system, or a combination of several more conventional processes cannot be answered from these results. We must wait for the results of other investigations, such as the recoil studies[43] and the on-line counter-telescope experiment[23] to further elucidate the mechanism(s) and resolve the ambiguities of the production of these light fragments from heavy targets.

ACKNOWLEDGMENTS

We would like to express our gratitude to E. Norton, J. K. Rowley, and R. W. Stoenner for performing chemical analyses on the samples. We have benefited much from the helpful and stimulating discussions with J. B. Cumming, S. Katcoff, and L. P. Remsberg. The cooperation of the operating staffs at the Brookhaven Cosmotron and Alternating Gradient Synchrotron is also hereby acknowledged.

*Research performed under the auspices of the U. S. Energy Research and Development Administration.

†Present address: Division of Laboratories and Research, New York State Department of Health, Albany, New York 12201.

[1]P. C. Stevenson, H. G. Hicks, W. E Nervik, and D. R. Nethaway, Phys. Rev. 111, 886 (1958).

[2]G. Rudstam and A. C. Pappas, Nucl. Phys. 22, 468 (1961).

[3]W. F. Biller, University of California Radiation Laboratory Report No. UCRL-2067 (unpublished).

[4]A. P. Vinogradov, I. P. Alimarin, V. I. Baranov, A. K. Lavrukhina, T. V. Baranova, F. I. Pavlotskaya, A. A. Bragina, and Yu. V. Yakovlev, Conference of the Academy of Sciences, USSR on Peaceful Uses of Atomic Energy, July 1-5, 1955; Session of Division of Chemical Sciences (unpublished), pp. 97, 132 [English translation by Consultants Bureau, New York, U.S. Atomic Energy Commission Report No. TR-2435, Pt. 2, 1956 (unpublished), pp. 65, 85].

[5]B. D. Pate, J. S. Foster, and L. Yaffe, Can. J. Chem. 36, 1691 (1958).

[6]G. Friedlander, L. Friedman, B. Gordon, and L. Yaffe, Phys. Rev. 129, 1809 (1963).

[7]R. Wolfgang, E. W. Baker, A. A. Caretto, J. B. Cumming, G. Friedlander, and J. Hudis, Phys. Rev. 103, 394 (1956).

[8]G. Friedlander, in *Proceedings of the Symposium on the Physics and Chemistry of Fission, Salzburg, Austria, 1965* (International Atomic Energy Agency, Vienna, 1965), Vol. II, p. 265.

[9]H. Ravn, J. Inorg. Nucl. Chem. 31, 1883 (1969).

[10]Ø. Scheidemann and N. T. Porile, Phys. Rev. C 14, 1534 (1976).

[11]J. M. Alexander, C. Baltzinger, and M. F. Grazdik, Phys. Rev. 129, 1826 (1963).

[12]G. Rudstam and G. Sørensen, J. Inorg. Nucl. Chem. 28, 771 (1966).

[13]E. Hagebø, J. Inorg. Nucl. Chem. 29, 2515 (1967).

[14]R. Brandt, in *Proceedings of the Symposium on the Physics and Chemistry of Fission, Salzburg, Austria, 1965* (see Ref. 8), Vol. II, p. 329.

[15]J. A. Panontin and N. T. Porile, J. Inorg. Nucl. Chem. 30, 2027 (1968).

[16]J. A. Panontin and N. T. Porile, J. Inorg. Nucl. Chem. 32, 1775 (1970).

[17]E. Hagebø, J. Inorg. Nucl. Chem. 32, 2489 (1970).

[18]K. Beg and N. T. Porile, Phys. Rev. C 3, 1631 (1971).

[19]L. P. Remsberg, F. Plasil, J. B. Cumming, and M. L. Perlman, Phys. Rev. 187, 1597 (1969).

[20]L. P. Remsberg, F. Plasil, J. B. Cumming, and M. L. Perlman, Phys. Rev. C 1, 265 (1970).

[21]L. P. Remsberg and D. G. Perry, Phys. Rev. Lett. 35, 361 (1975).

[22]D. G. Perry and L. P. Remsberg, Nucl. Instrum. Methods 135, 103 (1976).

[23]L. P. Remsberg (private communication).

[24]G. Friedlander and L. Yaffe, Phys. Rev. 117, 578 (1960).

[25]E. Hagebø and H. Ravn, J. Inorg. Nucl. Chem. 31, 897 (1969).

[26]L. Husain and S. Katcoff, Phys. Rev. C 7, 2452 (1973).

[27]S. Katcoff, H. R. Fickel, and A. Wyttenbach, Phys. Rev. 166, 1147 (1968).

[28]G. English, N. T. Porile, and E. P. Steinberg, Phys. Rev. C 10, 2268 (1974).

[29]G. English, Y. W. Yu, and N. T. Porile, Phys. Rev. C 10, 2281 (1974).

[30]J. B. Cumming, P. E. Haustein, R. W. Stoenner, L. Mausner, and R. A. Naumann, Phys. Rev. C 10, 739 (1974).

[31]J. B. Cumming, Annu. Rev. Nucl. Sci. 13, 261 (1963). The updated monitor cross section for 28.5 GeV is 8.0 mb [J. B. Cumming (private communication)]. However, for the sake of convenience and consistency with the published data, the value of 8.6 mb is used in this work.

[32]The appropriate reports in the *Nuclear Science Series on Radiochemistry of the Elements* [National Academy of Sciences-National Research Council. Reports No. NAS-NS-3020 and No. NAS-NS-3011 (unpublished)].

[33]C. M. Lederer, J. M. Hollander, and I. Perlman, *Table of Isotopes* (Wiley, New York, 1967), 6th ed.

[34]Nuclear Data Group, Nucl. Data B1–B6 (1966)–(1971).

[35]J. B. Cumming, National Academy of Sciences Report No. NAS NS-3107, 1962 (unpublished), p. 25.

[36]J. R. Grover, Phys. Rev. 126, 1540 (1962), footnote No. 13.

[37]Y. Y. Chu, E.-M. Franz, and G. Friedlander, Nucl. Phys. B40, 428 (1972).

[38]J. B. Cumming, R. W. Stoenner, and P. E. Haustein, Phys. Rev. C 14, 1554 (1976).

[39]J. Hudis and S. Katcoff, Phys. Rev. C 13, 1961 (1976).

[40]G. Rudstam, Z. Naturforsch. 21a, 1027 (1966).

[41]A. A. Caretto, J. Hudis, and G. Friedlander, Phys. Rev. 110, 1130 (1958).

[42]Y. Y. Chu, E.-M. Franz, G. Friedlander, and P. J. Karol, Phys. Rev. C 4, 2202 (1971).

[43]J. B. Cumming (private communication).